# MÖSSBAUER AND MAGNETIC PROPERTIES OF HEUSLER ALLOYS

D. Price, J. Rush, C. Johnson, M. Thomas, P. Webster

# MÖSSBAUER AND MAGNETIC PROPERTIES OF HEUSLER ALLOYS

D. C. PRICE

Dept. of Solid State Physics, Research School of Physical Sciences
Australian National University, Canberra, Australia

J. D. RUSH, C. E. JOHNSON, M. F. THOMAS

Dept. of Physics, University of Liverpool, Liverpool, U. K.

and

P. J. WEBSTER

Dept. of Pure and Applied Physics, University of Salford, Salford, U. K.

**Résumé.** — Ce travail discute les modèles théoriques qui sont couramment utilisés pour décrire le couplage magnétique entre les ions Mn, ainsi que les champs magnétiques hyperfins au siège de ions non magnétiques s, p présents dans les alliages $X_2MnZ$ de Heusler. Il montre que les données expérimentales sur la dépendance spatiale de l'interaction d'échange entre ions Mn-Mn dans $Pd_2MnSn$, sont consistantes avec le mécanisme oscillatoire à longue distance d'action, qui résulte de la diffusion des moments magnétiques de deux ions Mn par le potentiel d'un électron de conduction de type s (couplage à double résonance). Aucune évidence précise n'a été trouvée, qui soit en faveur d'un autre mécanisme plausible de couplage.

Le travail passe en revue les modèles actuels, qui impliquent des effets ioniques locaux dans la production de champs magnétiques hyperfins au siège des ions Z non magnétiques. L'étude se concentre tout spécialement sur deux modèles qui décrivent les champs en termes de la structure électronique locale du ion, et des raisons sont avancées pour justifier cette approche. La nature approximative de ces modèles est mise en évidence, ainsi que l'inopportunité conséquente de leur usage au vue d'établir des comparaisons détaillées avec l'expérience. L'accent est mis sur le besoin de davantage d'études théoriques détaillées, en vue d'établir ces modèles sur une base rigoureuse pratique et susceptible d'être perfectionnée.

Les mesures de l'effet Mössbauer qui sont rapportées dans ce travail concernent les ions $^{119}Sn$ et $^{121}Sn$ dans les solutions solides des alliages $Pd_2MnIn$, $Pd_2MnSn$ et $Pd_2MnSb$ de Heusler. La comparaison de ces données Mössbauer avec celles qui sont obtenues par diffraction de neutrons dans les alliages renfermant moins d'électrons que $Pd_2MnSn$, montre que les différentes structures magnétiques qui sont observées dépendent très sensiblement du nombre moyen d'électrons au siège de l'ion Z. Le mécanisme de couplage magnétique à double résonance s'avère être, au moins qualitativement, consistant avec ces observations.

Dans les alliages de composition $Pd_2MnSn_xSb_{1-x}$, les champs hyperfins, au siège des ions $^{119}Sn$ et $^{121}Sb$, changent rapidement avec le paramètre de composition $x$, quand $x$ s'approche de zéro. Ces propriétés sont discutées en termes des modèles mentionnés précédemment. Quant aux alliages dont la densité électronique approche celle de $Pd_2MnSb$, on n'observe ni champ hyperfin, ni variation de la température de Curie en fonction de $x$, qui soit explicable en termes du modèle des électrons libres des bandes de conduction. Des conclusions similaires sont déduites des measures de l'effet Mössbauer, concernant les ions $^{121}Sb$ dans les alliages $Pd_{1+y}MnSb$, quand $0 < y < 1$.

**Abstract.** — Theoretical models that are currently used to describe the magnetic coupling between Mn ions and the magnetic hyperfine interactions at non-magnetic s, p ions in $X_2MnZ$ Heusler alloys are discussed. Experimental data on the spatial dependence of the Mn-Mn exchange interaction in $Pd_2MnSn$ is shown to be consistent with the long-range oscillatory mechanism that arises from the potential scattering of an s-like conduction electron by two Mn moments — the double resonance coupling. No definite evidence is found for any other significant coupling mechanism.

Present models that involve local ionic effects in the production of the magnetic hyperfine fields at non-magnetic Z site ions are reviewed. Attention is concentrated on two models that describe the fields in terms of the local electronic structure of the ion, and reasons for this are given. Emphasis is placed on the approximate nature of these models and on the consequent inadvisability of using them for detailed comparisons with experiment. The need for more detailed theoretical work aimed at providing a rigorous basis for application and subsequent refining of these models is stressed.

$^{119}Sn$ and $^{121}Sb$ Mössbauer measurements have been made on solid solutions of the Heusler alloys $Pd_2MnIn$, $Pd_2MnSn$ and $Pd_2MnSb$. Comparison of Mössbauer data with neutron diffraction data for alloys with fewer electrons than $Pd_2MnSn$ shows that the different magnetic structures

that are observed depend very sensitively on the average number of electrons at a Z site ion. The double resonance magnetic coupling mechanism is seen to be at least qualitatively consistent with these observations.

For alloys with electron densities approaching that of $Pd_2MnSb$, rapid changes of both the $^{119}Sn$ and $^{121}Sb$ hyperfine fields with composition are observed. These are discussed in terms of the hyperfine field models previously described and, along with changes in this composition range in other quantities such as the Curie temperature, cannot be explained using the normal free electron-like description for the conduction band. Similar conclusions are drawn from $^{121}Sb$ Mössbauer measurements on solid solutions of PdMnSb and $Pd_2MnSb$.

1. **Introduction.** — In 1903 F. Heusler reported that it was possible to make ferromagnetic alloys from the non-ferromagnetic constituents copper-manganese bronze and group B elements such as aluminium and tin. These alloys, some of whose properties were reviewed by Webster [1], are of interest from several points of view. They are ternary compounds with a simple structure (Fig. 1) that consists of four inter-

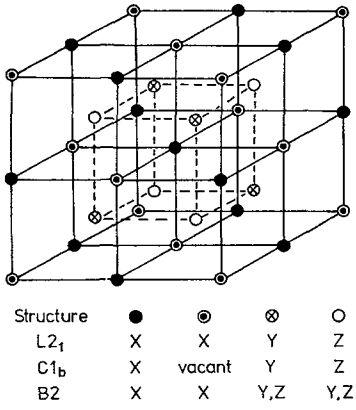


FIG. 1. — The Heusler structure, with the four f. c. c. sublattices indicated.

penetrating f. c. c. lattices which may be thought of as a b. c. c. CsCl-type structure in which alternate positions on each sublattice may be occupied by different atoms. Within the general Heusler classification there are three common structures corresponding to different arrangements of atoms on the four f. c. c. sublattices. These are indicated in figure 1 with their Strukturbericht labels. The stoichiometry of the $L2_1$ (which is the original Heusler structure) and B2 structures is $X_2YZ$ while that for the $Cl_b$ structure is XYZ. The constituents X, Y and Z may be any of a large number of elements and consequently there is a wide variety of different Heusler alloys. In general, and there are exceptions, X is a noble metal or a transition metal (3d, 4d or 5d) atom with an almost full outer d shell, Y is a transition metal atom with fewer outer d electrons than X, and Z is a non-transition metal atom.

Many Heusler alloys, in particular those with Co in the X site and/or Mn in the Y site, exhibit magnetic order with transition temperatures ranging up to several hundred K. Heusler's original ferromagnetic alloys contained Mn on the Y site of the $L2_1$ structure and it was shown that the magnetic properties were both structure and composition-dependent (see [1]). We shall restrict our attention in this paper to alloys with Mn on the Y sites as the only magnetic constituent (i. e. alloys containing no Co) in order to have a specific magnetic system on which to base our discussions. The magnetic properties of these alloys are of interest because the Mn atoms are well separated, so that direct exchange between them must be negligible, and appear to have well-localized magnetic moments [2]. Magnetic order has traditionally been assumed to be due to long-range interactions via the conduction electrons, but recent experimental results have been interpreted as indicating the presence of strong short-range interactions. The ordering temperatures, and in some cases even the type of order, depend strongly on the particular atoms occupying both the X and Z sites. Consequently, this class of compounds provides a simple and structurally well-defined system of magnetic moments in a widely variable environment in which to study the magnetic interactions.

Perhaps more important in the context of this Conference is the relevance of the large number of possible constituent atoms to the study of hyperfine field systematics and the origins of hyperfine fields in metals. Of particular interest is the number of s, p elements that can occupy the Z site and the apparent ease with which these can be substituted for one another, at least in small concentrations, in some alloys. There seems little reason to doubt that such substitution is restricted to the Z sites except, of course, in alloys of B2 structure. Campbell [3] has recently published a summary of hyperfine field measurements in pure and substituted Heusler alloys. We shall not attempt to duplicate this here.

Our aim in this paper will be to examine current theories of both the magnetic and hyperfine interactions in Heusler alloys, and to present some of our recent Mössbauer results on a system that has important implications in both of these areas. Although much of the interest in Heusler alloys stems from their well-defined structural characteristics we will not comment on possible reasons for these metallurgical properties : this appears to be an area that is not yet well understood.

The following two sections of this paper will deal briefly with theories of the magnetic properties of alloys of the type $X_2MnZ$ and XMnZ and of hyperfine

interactions in these alloys, particularly at Z site atoms. We shall then describe the results of some recent Mössbauer and magnetic measurements on the systems $Pd_2Mn$(In, Sn, Sb) and $Pd_{1+z}MnSb$ and relate them where possible to the theories described.

It is our opinion that there is now a good qualitative understanding, derived mainly from experiment, of the electronic and magnetic interactions in Heusler alloys. We feel that further significant advances will depend on purposefully planned experiments and on more detailed theoretical work being done in order to obtain a more rigorous basis for comparing current models with experiment.

2. **Magnetic coupling in Heusler alloys.** — 2.1 INTRODUCTION. — Prior to 1966 discussions of the magnetic interactions in Heusler alloys were either empirical or were qualitative and based, in general, on the RKKY theory of polarization of conduction electrons by the s-d exchange interaction [1]. The first model to give reasonable quantitative estimates of transition temperatures, even though employing the molecular field approximation, was that of Caroli and Blandin [4] (to be referred to as CB hereafter). The application of this model to Heusler alloys was also examined by Geldart and Ganguly [5], Brooks and Williams [6] and others. The model is based on the work of Caroli [7] and the coupling effectively arises from the scattering of a conduction electron by different Mn local moments. The scattering occurs as a result of the s-d mixing term in the Friedel-Anderson model [8] of the Mn localized moment. Caroli [7] estimated that, for the case of Mn in copper, this double resonance exchange coupling would be approximately two orders of magnitude larger than coupling due to s-d exchange.

Long-range magnetic coupling of localized moments via the conduction electrons was widely accepted as being the dominant exchange mechanism in Heusler alloys for some time. Recently, however, Ishikawa and Noda [9] have, using inelastic neutron scattering, measured the magnon dispersion curves of $Pd_2MnSn$ and $Ni_2MnSn$, and derived the distance dependence of the effective exchange integral $J(r)$ in these compounds. This excellent series of measurements has renewed interest in the theory of the magnetic coupling in Heusler alloys. The results show that coupling between Mn ions at relatively large separations (further apart than 3rd nearest neighbours) can be satisfactorily described by the CB model, but that at smaller separations it cannot : exchange of the wrong sign is predicted by the CB model between near neighbour (1nn) and second nearest neighbour (2nn) Mn ions. This prompted Kasuya [10] to suggest that a short-range ferromagnetic virtual double exchange mechanism might be present in addition to the long-range double resonance coupling.

Campbell and Stager [11] have measured the saturation magnetization and Curie temperatures of alloys based on $Ni_2MnSn$ in which some of the Mn ions are replaced by Ti, V or Cr ions. They interpreted their results to indicate that in these alloys the Ti ions carried a net moment of $\sim -1\ \mu_B$, the V ions were non-magnetic (zero moment) and Cr ions had a moment of $\sim +1\ \mu_B$. As a result of these measurements Campbell [12] has suggested, following Goodenough [13], that the dominant exchange process is a super-exchange interaction with the Z site s, p ion acting as the intermediary.

A shortcoming of the CB double resonance coupling model, the effects of which do not appear to have been quantitatively evaluated so far, is that it involves approximations that limit its range of applicability to ions that are separated by large distances i. e. it involves asymptotic formulae in the evaluation of certain integrals. We have recently done a calculation in the same spirit as CB but without the use of these asymptotic formulae. This calculation and its results will be described briefly below. As a result of it we believe that there are no experimental results presently available that cannot be explained (at least in principle) using double resonance coupling as the dominant exchange mechanism.

2.2 « EXACT » CALCULATION OF THE DOUBLE RESONANCE COUPLING. — Our model, which is based on the Hartree-Fock approximation, is the same as that of Caroli [7] and very similar to those discussed in some detail by Moriya [14] and Kim and Nagaoka [15]. We start from the Anderson Hamiltonian [8] generalized to the case of two impurities :

$$\mathcal{H} = \sum_k \varepsilon_k n_k + \sum_{mi\sigma} \left\{ \varepsilon_{m_i} n^{\sigma}_{m_i} + \sum_k V_{m_i k}(C^*_{k\sigma} C_{m_i\sigma} + C^*_{m_i\sigma} C_{k\sigma}) + \frac{U}{2} \sum_p n^{\sigma}_{m_i} n^{-\sigma}_{p_i} + \frac{U-J}{2} \sum_{p\neq m} n^{\sigma}_{m_i} n^{\sigma}_{p_i} \right\} \quad (1)$$

where the notation is standard (see [7], [14]). $m$, $p$ are localized orbitals on impurity i. $V_{m_i k}$ is the s-d mixing matrix element between the localized state $m$ on impurity i and the state $k$ of the conduction band. A direct d-d interaction term should also be included in (1) but we have neglected it on the grounds that the magnetic atoms are well separated. This ignores the possibility that d-d admixture with the neighbouring transition metal ions on the X sites is important, and this should be borne in mind.

In the limit of isolated magnetic ions (i. e. no interaction between them) this Hamiltonian gives rise to the familiar virtual bound state picture for the localized orbitals, and a magnetic moment is formed if the effective exchange energy $(U + 4J)$ is sufficiently large compared with the width $\Delta_m$ of this state ([8], [14] and [16]). The

interaction between two magnetic ions is manifested firstly as a change in the magnitude of the localized moment on each and secondly as a coupling between them. The former has been considered qualitatively by Kim and Nagaoka [15] and by Moriya [14] and may be relevant to the interpretation of the results of Campbell and Stager [11]. We will concentrate on the latter effect here.

If $\delta\rho_T^\sigma(\varepsilon)$ is the change in the total density of electron states of spin $\sigma$ caused by the interaction between magnetic ions, then the interaction will produce a decrease in the total energy of the system given by [7] :

$$E_{\text{int}} = \operatorname*{Tr}_{\text{spins}} \left\{ \int_{-\infty}^{E_F} (\varepsilon - E_F)\, \delta\rho_T^\sigma(\varepsilon)\, d\varepsilon - U \sum_{m,i} n_{0m_i}^\sigma\, \delta n_{m_i}^{-\sigma} \right\} \tag{2}$$

where $n_{0m_i}^\sigma$ is the occupation number of the localized state of spin $\sigma$ in orbital $m$ on ion i in the absence of the ion-ion interaction and $\delta n_{m_i}^\sigma$ is its change due to the interaction. The following assumptions are made in the evaluation of $E_{\text{int}}$ :

(i) For the case of a pure Mn magnetic lattice we take all of the magnetic ions to be identical.

(ii) Following Caroli [7] we take the $\delta n_m^\sigma$ to be small and neglect the second term in (2).

(iii) The different d orbitals on a magnetic ion are taken to be equivalent, apart from their angular momentum properties.

Then, in terms of the Green's functions $G_{dd}^{0\sigma}(\varepsilon, n)$ for the Mn d states in the absence of the interaction between ions, the expression (2) reduces to :

$$E_{\text{int}}(R) \approx -\frac{1}{\pi} \operatorname{Im} \operatorname*{Tr}_{\text{spins}} \sum_m \int_{-\infty}^{E_F} G_{dd}^{0\sigma}(\varepsilon, n_0)\, F_m(\varepsilon, R)\, G_{dd}^{0\sigma}(\varepsilon, n_0)\, d\varepsilon \tag{3}$$

where

$$F_m(\varepsilon, R) = \left( \sum_k \frac{V_{m_i k}\, V_{k m_j}}{\varepsilon + is - \varepsilon_k} \right)^2 \qquad (s \to 0)$$

$$G_{dd}^{0\sigma} = -\frac{1}{\Delta} \sin \delta^\sigma(\varepsilon) \exp[i\delta^\sigma(\varepsilon)]$$

$\delta^\sigma(\varepsilon)$ is the d-like phase shift of an electron of spin $\sigma$ and energy $\varepsilon$ that is scattered by the Mn ion potential.

The evaluation of the matrix elements $V_{m_i k}$ and $V_{k m_j}$ is important as it is from them that the $R$-dependence of $E_{\text{int}}$ is derived. If the ion i is taken to be at the origin and $j$ is at $\mathbf{R}$, then

$$V_{m_i k} = \langle \varphi_m^i(\mathbf{r}) \mid V_i(\mathbf{r}) \mid \mathbf{k} \rangle$$

$$V_{m_j k} = \langle \varphi_m^i(\mathbf{r} - \mathbf{R}) \mid V_j(\mathbf{r} - \mathbf{R}) \mid \mathbf{k} \rangle .$$

As $\varphi_m(\mathbf{r})$ is an atomic-like function and is written as $R_l(r)\ Y_l^m(\hat{r})$, and the conduction band states are approximated by plane waves, the expressions for $V_{m_i k}$ and $V_{m_j k}$ reduce to :

$$V_{m_i k} = \frac{1}{\sqrt{N}} V(k)\, Y_l^{m*}(\hat{\mathbf{k}})$$

$$V_{m_j k} = \frac{e^{i\mathbf{k}.\mathbf{R}}}{\sqrt{N}} V(k)\, Y_l^{m*}(\hat{\mathbf{k}}) \tag{4}$$

with

$$V(k) = 4\pi i^l \int_0^\infty R_l^*(r)\, V(r)\, j_l(kr)\, r^2\, dr .$$

The integral in (3) is then evaluated numerically assuming that $V(k)$ can be approximated by its value at $k_F$. (This can be justified if the dominant contributions to the integral in (3) come from the region near $E_F$.) Caroli [7] evaluated it analytically in the asymptotic limit, which is equivalent to ignoring the spherical harmonics in (4) i. e. no account was taken of the d symmetry of the scattering of the Mn ion. Alloul [16] pointed out that this was also the important difference between asymptotic and non-asymptotic expressions for the spin polarization induced by a magnetic moment in the conduction band. The results obtained are exact only in the sense that the evaluation of (3) is exact (apart from the $k$-dependence of $V$). The model from which the expression (3) is derived contains a number of approximations, only some of which have been explicitly mentioned.

The effective exchange integral J is derived from $E_{\text{int}}$ as

$$J = -\frac{1}{4S^2} E_{\text{int}} ,$$

where $S$ is the effective spin of a Mn ion.

2.3 Results of calculation. — The solid line in figure 2 was calculated as described above, and the experimental results of Ishikawa and Noda [9] for $Pd_2MnSn$ are seen to be satisfactorily described by it. It was assumed in the calculation of this curve that the spin-up 3d states of each Mn ion were fully occupied

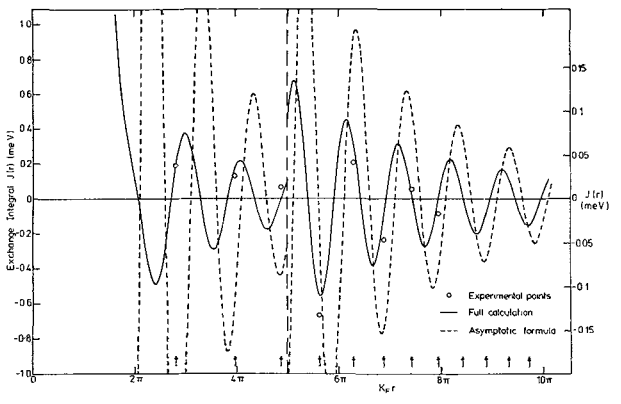


FIG. 2. — The effective exchange integral $J(r)$ between two Mn ions separated by distance $r$. The experimental points were determined from the magnon dispersion curves of $Pd_2MnSn$ by Ishikawa and Noda [9], and are plotted as a function of $k_F r$ using the value $k_F = 1.0$ a. u. The solid line is calculated, as described in the text, from the double resonance model of Caroli [7] but without making any asymptotic approximations. The parameters used to describe local Mn states are given in the text. The dashed curve is calculated, using the same set of parameters, from the asymptotic formula of Caroli. Note the change in the scale of the ordinate that occurs at the vertical dashed line.

and that the net moment per ion was 4.2 $\mu_B$ as observed for $Pd_2MnSn$ [2]. The width $\Delta$ of the spin down 3d states was taken rather arbitrarily to be $\sim E_F/10$ with $E_F \sim 0.40$ a. u. (= 10.9 eV). Using these parameters the calculated curve described the experimental points best for a value of $k_F$ of $\sim 1.0$ a. u. (= 1.9 Å$^{-1}$) and $V(k_F)$, which was used to scale the curve vertically, about 7 % larger than its value calculated from a free electron approximation [16]. The value of $k_F$ is $\sim$ 20 % larger than is normally assumed from standard prescriptions of the number of conduction electrons contributed by each atom (see, e. g., [4], [5], [6], [10], [17]) but we do not regard this as being serious for two reasons. Firstly, and most importantly, it must be emphasized that the calculation reported here contains a number of potentially important approximations. Apart from those mentioned both explicitly and implicitly in the last section it will be appreciated that the coupling considered is that between a single pair of magnetic ions and as such takes no account of the effects of other neighbouring and intervening ions. It should be more appropriate to a dilute alloy situation than to the case here of a concentrated magnetic material. Because of all the approximations involved we feel that any numerical results obtained should not be taken too seriously. Secondly, in the absence of any calculation or direct measurement of the structure of the conduction band in these alloys it is difficult to regard this value of $k_F$ as being obviously unreasonable. One interpretation of the results that will be presented below (Section 6) is that the conduction band is much more complicated, at least in some alloys, than a free electron band.

The dashed curve in figure 2 is the exchange parameter $J(r)$ calculated from the asymptotic formula of CB [4] for the same values of the parameters used for the solid curve. The asymptotic formula neglects terms of higher powers of $1/r$ which is why it predicts a much larger coupling at small $r$ values than does the non-asymptotic calculation. The arrows at the bottom of figure 2 indicate the positions, for the value of $k_F$ used, of the successive Mn coordination shells.

We hope to give further details of this calculation and its results in a future publication.

2.4 DISCUSSION. — Because the results reported here contain a number of potentially serious approximations it is probably not reasonable to base any firm conclusions on them. However, we feel that they give an indication that the s-d mixing mechanism may be primarily responsible for the exchange interactions in Heusler alloys such as $Pd_2MnSn$, or at least that more detailed calculations should be carried out before other exchange mechanisms are assumed to be necessary.

We feel that, at least in principle, it is possible to qualitatively account for the results of Campbell and Stager [11] in terms of this exchange mechanism although no numerical results have yet been obtained. An isolated Ti ion, for example, would be assumed to carry no localized moment, as is the case in its dilute alloys with noble and other metals [18], [19], and the effect of its interaction with surrounding Mn ions via the s-d mixing mechanism would be to reduce their moment. This sort of effect has been discussed by Moriya [14] and Kim and Nagaoka [15]. These latter authors show qualitatively that for a case such as Mn substituted for Ti in $Ni_2TiSn$, the Mn moment should increase as the Mn concentration increases, as is observed [11].

It will be shown below (Section 5) that the s-d mixing exchange as described here can account for changes in magnetic order with conduction electron density that are qualitatively similar to those observed in the alloy systems $Pd_2MnIn_{1-x}Sn_x$ ($0 \leqslant x \leqslant 1$) and $Pd_2MnIn_{1-y}Sb_y$ ($0 \leqslant y \leqslant 0.5$).

3. **Hyperfine fields in Heusler alloys.** — 3.1 INTRODUCTION. — At the current stage of development of understanding of the origins of magnetic hyperfine fields in metals it is desirable to establish the systematics of these fields in systems that are as simple as possible. The s, p ions in the Z sites of $X_2MnZ$ (or XMnZ) Heusler alloys constitute such a simple system : the alloys are cubic, their magnetization is localized on the Mn ions and there would appear to be very little direct overlap of the Z site ion with the Mn 3d electrons that carry the magnetic moment. Because we feel that this is the main reason for studying hyperfine fields in Heusler alloys instead of, say, dilute binary alloys or other intermetallic compounds, we shall restrict our attention here to this system. There is,

however, a growing interest in hyperfine fields at transition metal ions in the X sites of Heusler alloys and also in the fields at all ions in alloys containing cobalt when it carries a magnetic moment. Such measurements would, we feel, be more properly included in a more general review of hyperfine fields in metals.

A large number of measurements have now been made of hyperfine fields of non-magnetic ions in Heusler alloys. These have recently been summarized by Campbell [3], and definite trends are becoming evident. Campbell's paper should be consulted for references to specific measurements where they are not given here.

Historically, measurements were first made on pure Heusler alloys such as $Cu_2MnAl$, $Cu_2MnSn$, $Ni_2MnSn$, $Pd_2MnSn$ and the first attempt at explaining them was made by Caroli and Blandin [4] in the same paper in which they discussed the magnetic coupling. They assumed that the hyperfine field at a non-magnetic ion reflected only the polarization of the conduction electrons at its site through the Fermi contact interaction. However, following the important step of Leiper and Campbell [20], [21] and Swartzendruber and Evans [22] of measuring the fields at non-magnetic ions substituted into Heusler alloy Z sites, it rapidly became clear to most people that there was a strong dependence of the hyperfine field on the particular ion at which it was measured, and that this could not be described by the Caroli-Blandin model. Figure 3

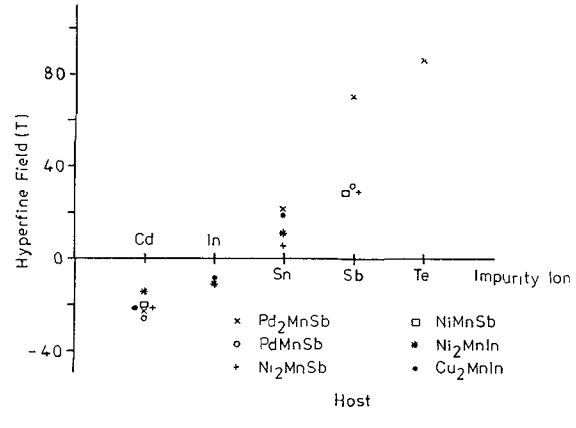


FIG. 3. — Hyperfine fields at 5s, p ions in the Z sites of the Heusler alloy hosts indicated. This shows that, with the possible exception of $Pd_2MnSb$, there is only a relatively weak dependence of the field on the particular host compared with the dependence on the ion at which the field is measured. These measurements have been taken directly from the literature (see [3] for references) and no corrections (for example to $T = 0$) have been made.

illustrates this dependence : it can be seen that the hyperfine fields vary in a qualitatively similar way from ion to ion with relatively little change with host (except in the case of $Pd_2MnSb$). There was, therefore, a necessity to account for the local properties of a particular ion (which had been recognized for some time in the case of dilute impurities in binary alloys [23]) although it was not immediately obvious which local properties had to be taken into account.

Three different models have subsequently been proposed that incorporate local ionic effects. In one, Stearns [24] proposes that it is the ionic volume, or more strictly its misfit in the host lattice, that is important. In the others of Blandin and Campbell [25] and Jena and Geldart [17] it is considered that the effects of the local electronic structure dominate. These models and their applicability will be discussed below.

3.2 STEARNS' VOLUME MIS-FIT MODEL. — This model was originally proposed [24] to account for the hyperfine field variations at impurity ions in Fe, Co and Ni, although we understand that its applicability to Heusler alloys is under consideration [26]. It is an empirical model that makes use of a similarity between the variations of impurity hyperfine fields and atomic volumes. The hyperfine field at a non-magnetic impurity is assumed to consist of two contributions. One is from the host spin polarization in the same spirit as the Caroli-Blandin model while the other is proportional to the volume mis-fit of the impurity in the host.

We doubt that this model represents the physical situation in either binary alloys or Heusler alloys as it does not appear capable of explaining in a consistent way several experimental results. Some inconsistencies have been mentioned by Campbell and Vincze [27] although Stearns has replied to these [28]. Other points of difficulty for this model would appear to be explanations of :

(i) the pressure dependence of the hyperfine field at Sn in iron. Möller [29] showed that the negative hyperfine field became much more strongly negative as the lattice was compressed ;

(ii) the temperature dependence of the hyperfine fields at non-magnetic impurities in iron, and in particular that of the field at As compared with other impurities [30] ;

(iii) the calculations of Sondhi [31] of the overlap between the orbitals of solute s electrons and 3d electrons of iron in dilute iron alloys. These indicate that the direct overlap is an order of magnitude too small to explain the volume mis-fit field in binary alloys. In Heuslers, where the separation between the Mn ions and Z site ions is even larger, it is difficult to see that direct overlap could be significant ;

(iv) it will be shown in section 6 below that some of our measurements on alloys near to the composition $Pd_2MnSb$ cannot reasonably be explained using the volume mis-fit model. Other measurements in $Pd_2MnSb$ [42], [49], [50], [51], [52] also do not vary in the same way as the impurity atomic volume.

3.3 BLANDIN-CAMPBELL MODEL. — This model represents a modification of the Caroli-Blandin model [4] in order to take account of the effect of the electronic structure in the conduction band in the immediate vicinity of the impurity. It should be recognized at once that in principle it cannot be regarded as being strictly applicable to a concentrated magnetic material since, in common with the Caroli-Blandin model, it considers isolated pairs of atoms in an unpolarized electron sea (see Section 2 above). However, since the effects of coherent scattering and other effects of neighbouring ions are not well known, the model may be empirically useful. It has the advantage that the effect of the non-magnetic ion is included explicitly as the phase shifts it produces in scattered electrons, so that realistic impurity potentials can be readily employed.

As originally formulated by Blandin and Campbell [25] the model contained several numerical approximations. These are not essential to the spirit of the model and were presumably made in order to give a qualitative indication in simple terms of the expectations of the model. In particular, Blandin and Campbell only accounted in a very approximate way for the spin polarization produced by a Mn ion that is a near neighbour to a non-magnetic ion and they used only a rough estimate of the $l = 0$ phase shifts produced by the non-magnetic ion. Unfortunately the model has sometimes been criticized on the basis of these numerical approximations (e. g. [3], [51]) and, whilst acknowledging that the usefulness of a model calculation lies in it being simpler than an *ab initio* one, we do not believe this criticism to be justified in this case in the absence of a more detailed numerical examination. An example of the effect of a simple variation in one of these aproximations is shown in figure 4. The predictions of the Blandin-Campbell model applied to a typical $X_2MnZ$ Heusler alloy are given for impurity phase shifts calculated by

$$\delta_0 = \frac{\pi Z_{sc}}{4},$$

where $Z_{sc}$ is the excess charge to be screened, and for phase shifts calculated if the impurity potential was a spherically symmetric square well satisfying the Friedel sum rule. The differences between these curves illustrate the inadvisability of making detailed comparisons of experimental results with qualitative model calculations.

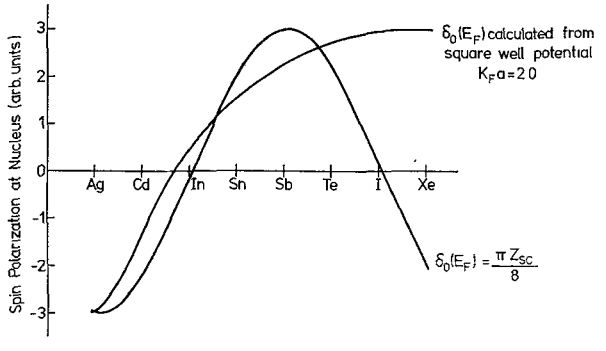


FIG. 4. — The effect of varying one of the numerical approximations used in the Blandin-Campbell model for hyperfine fields of s, p ions in Heusler alloys. All parameters other than the $l = 0$ phase shifts at the Fermi level, $\delta_0$, are the same as those used by Campbell and Blandin [25]. The calculated electronic spin polarization at the non-magnetic ion nuclei is shown when their simple approximation $\delta_0 = \pi Z_{sc}/4$, where $Z_{sc}$ is the impurity charge to be screened, is used and when the phase shifts are calculated assuming that the ionic potential is a spherically symmetric square well that satisfies the Friedel sum rule.

3.4 JENA-GELDART MODEL. — In 1963 Daniel and Friedel [23] calculated the electron spin polarization at the nucleus of a non-magnetic ion dissolved in an explicitly spin-polarized electron sea, and applied it to the case of dilute impurities in ferromagnetic binary alloys. The principle on which their calculation was based was that, since the impurity ion potential was non-magnetic and the density of conduction electrons in the host was different for the two spin directions, electrons of opposite spin would be scattered differently by the non-magnetic ion. They used the simplest model possible to illustrate this principle : the impurity ion was represented by a spherically symmetric square-well potential whose radius was that of the Wigner-Seitz sphere of the ion and whose depth was calculated to satisfy the Friedel sum rule. The conduction electrons of the host metal, which were taken to behave as free electrons, were assumed to have a uniform spin polarization within this Wigner-Seitz sphere. The conduction band contained all the effects of the host. Jena and Geldart [32] have given a more fundamental derivation of these approximations.

Swartzendruber and Evans [33] first suggested that this model might be applicable to Heusler alloys but it was left to Jena and Geldart [17], [32] to make detailed comparisons of its predictions with measured hyperfine fields. The Jena-Geldart model is identical to that of Daniel and Friedel in principle and only varies numerically by the use of an othogonalized plane wave approximation for calculating the wave functions of the Bloch electrons in the vicinity of the nucleus. Some results of the model are illustrated in figure 5 (we note some minor numerical discrepancies with the results of Jena and Geldart in the caption). The quantity $f$ that is plotted in figure 5 against the valence $Z_I$ of the ion is a dimensionless quantity that is defined by Daniel and Friedel [23]. It is proportional to the spin polarization at the nucleus of the ion and its value depends only on $Z_{sc}$, the charge to be screened that depends on the ionic potential, and $k_F\, a$, where $k_F$ is the wave number for conduction electrons at the Fermi surface and $a$ is the radius of the square potential well used to approximate the ion's potential. The values of $k_F\, a$ appropriate to each curve are indicated on the figure.

This model has the conceptual advantage that it is

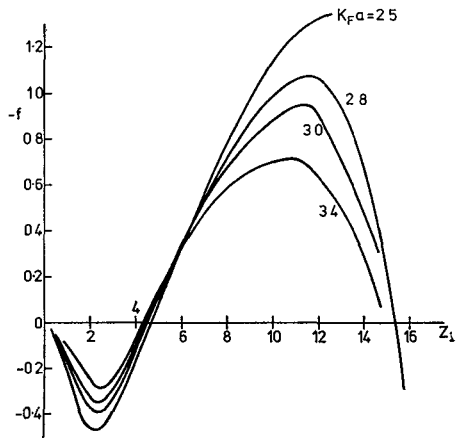


FIG. 5. — Spin polarization calculated from the Daniel-Friedel model. The quantity f is proportional to the electronic spin polarization at the nucleus of an ion with valence $Z_I$, and is defined by Daniel and Friedel [23]. The value of the parameter $k_F a$, defined in the text, that is appropriate to each curve is indicated. In comparing these curves with those in the paper of Jena and Geldart [17] it will be seen that there is a difference in the points at which the curves cross the $Z_I$ axis. This appears to be due to a numerical discrepancy that is still unresolved, although we do not regard it too seriously in view of our comments in the text about the purely qualitative applicability of these models. It may be noted that our calculations, some of which are shown above, agree with those of Daniel and Friedel [23] and of Koenig [35]. Another point concerning the paper of Jena and Geldart [17] is that their published polarization curves (their Fig. 1) are calculated using the value $\Delta/E_F = 0.01$ for the relative splitting of the conduction band. This is not mentioned in their paper and account must be taken of it in calculating hyperfine fields from their work. This is done by normalizing to the phenomenologically determined value of $\Delta/E_F$.

formulated specifically for a concentrated magnetic material and includes all the effects of coherent scattering, exchange, hybridization, etc. automatically through a parameter that is determined phenomenologically. A disadvantage is that it requires a rather detailed knowledge of the ion's potential and consequently is difficult to adapt to more realistic ionic potentials : the form of the potential is expected to become increasingly important for higher values of $Z_I$ when bound states are present. The model may also be expected to have difficulty for very small values of $Z_{sc}$ when the potential is of the same order as the spin splitting of the conduction band. Jena and Geldart [32] have examined this region using perturbation techniques, however, and find qualitative agreement with the Daniel-Friedel results.

3.5 COMPARISONS AND APPLICABILITY OF THE MODELS. — Campbell and Vincze [27] and Watson and Bennett [34] have pointed to the ambiguity involved in the correlation of impurity hyperfine field values with various atomic quantities, since this may simply indicate a relationship between these quantities without implying which one is responsible for the basic physical mechanism. For example, the atomic volume of an impurity ion is related to its electronic structure, and therefore to its valence and screening characteristics, because both depend on the nuclear charge and the electron-electron interactions within the ion. In her papers, Stearns [24] has simply drawn attention to the correlation between hyperfine field and impurity volume and has only by implication suggested that it represents directly the physical mechanism responsible for the observed hyperfine fields. We disagree for the reasons mentioned in 3.2 above.

These considerations also mean, of course, that because the models based on local electronic structure can show the same qualitative trends as the experimental results, they do not necessarily represent the underlying physical origins of the hyperfine fields either. However, these models predict, in a qualitatively correct way, the form that the hyperfine field vs. ionic valence correlation should take, and they also incorporate what appears to be a plausible physical process which, for lack of a reasonable alternative, we shall take to represent the actual mechanism that gives rise to the observed hyperfine fields. It should be appreciated that a realistic calculation of hyperfine fields at ions in metals based on the principle that local electronic screening and its interaction with the spin-polarized electrons in the host is the process responsible for them, would be extremely complex so, at least in the near future, it is unlikely that the supposedly dominant role played by this mechanism will be conclusively confirmed or denied.

We now turn our attention to the models describing this process proposed by Blandin and Campbell [25] and Jena and Geldart [17] and briefly described above. These two models are complementary in that they start from rather diverse propositions. Both, at their present stage of development, appear to describe the observed trends in hyperfine field systematics for non-magnetic ions in a qualitatively reasonable way. However, we wish to emphasize that in view of the approximations employed in their derivation it is difficult to justify any detailed comparison of their predictions with the experimental results. Some of these approximations have already been mentioned. A central problem is the lack of a sound basis for assigning values for the parameters used in the models, such as $k_F$ and $Z_{sc}$, particularly for materials such as Heusler alloys that might be expected to have a fairly complicated band structure and in which the s, p ions are constituents of the lattice. This problem has been pointed out by Campbell and Blandin [25]. Because of the relatively large body of data that exists (e. g. [3]) and because models that can qualitatively account for it exist, we feel that a theoretical effort aimed at characterizing the electronic energy bands in these alloys can now be justified. Experimental work may also be better directed towards the determination of properties that would provide other points of contact for theory e. g. transport properties, specific heats, spectroscopic properties.

**4. Some recent experimental results : general remarks.** — The remainder of the paper will be devoted to a rather brief review of some of our recent $^{119}Sn$ and $^{121}Sb$ Mössbauer measurements on the Heusler systems $Pd_2Mn(In, Sn, Sb)$ and $Pd_{1+z}MnSb$. This work will soon be submitted for publication in more complete form so we will give here only those experimental details that are necessary to this discussion.

There is a certain amount of work on Heusler alloys in the literature that appears to be in error because the alloys measured were not properly characterized. This is most important, as many alloys do not form a Heusler phase at all, or exist only as a mixture of phases. Mixed alloy systems do not always form good solid solutions even when the end members are well-behaved. Consequently, measurements should only be reported when there are sound reasons, backed by X-ray and, where possible, neutron diffraction evidence to indicate that the alloys concerned are single phase Heusler structure and, where appropriate, are good solid solutions. The alloys that we will discuss below have been characterized in this manner. Details will be reported [36].

4.1 FITTING THE MÖSSBAUER SPECTRA : P(H) DISTRIBUTIONS. — The spectra we will discuss are assumed, in general, to result from nuclei (either $^{119}Sn$ or $^{121}Sb$) that experience a distribution $P(H)$ of magnetic hyperfine fields $H$ owing to their different local environments in a particular alloy. The forms of these distributions were determined from the Mössbauer spectra in the manner described by Window [37] i. e. the distribution was approximated by a sum of harmonic components with fixed boundary conditions. The number of harmonics that are required to satisfactorily approximate the distribution depends on its shape, while the number that can be meaningfully determined depends on the statistical quality of the measured spectra. These two competing considerations often mean that what should be sharp $P(H)$ distributions will contain oscillations whose frequency will be that of the highest harmonic used : care must be taken that such oscillations are not interpreted as genuine features of the $P(H)$ distribution.

In determining these $P(H)$ distributions it was assumed, in general agreement with measurements made at room temperature when the alloys are paramagnetic, that all similar nuclei in a sample have the same isomer shift and experience zero electric field gradient. This latter condition was probably not rigorously satisfied in some alloys, but the effects of quadrupole interactions were generally small enough that the $P(H)$ distribution provided a meaningful description of the major features of the Mössbauer spectrum from which it was derived. It should be emphasized that our interest here will be only in the broad qualitative features of the spectra and, therefore, of the $P(H)$ distributions obtained from them.

Examples of $P(H)$ distributions derived from $^{119}Sn$ and $^{121}Sb$ Mössbauer spectra are shown in figure 6. The $^{119}Sn$ spectra are from the alloy $Pd_2MnIn_{0.4}Sn_{0.6}$ at 4.2 K with magnetic fields of 0, 3 T and 6 T applied

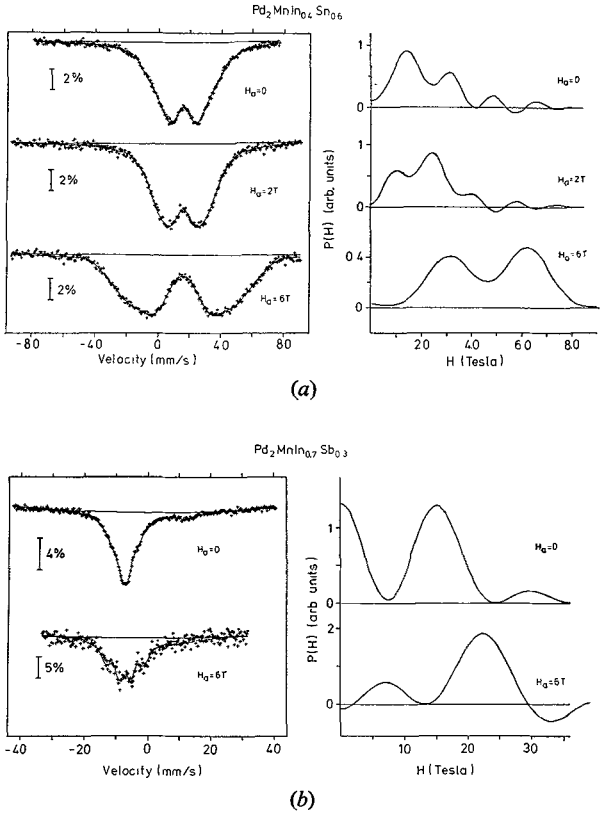


FIG. 6. — Examples of $^{119}Sn$ and $^{121}Sb$ Mössbauer spectra and of the $P(H)$ distributions derived from them as described in the text. The solid lines drawn through the spectra are produced by the $P(H)$ distributions shown : *a*) $^{119}Sn$ measurements on the alloy $Pd_2MnIn_{0.4}Sn_{0.6}$ at 4.2 K. The magnitudes of magnetic fields $H_a$ applied perpendicular to the $\gamma$-ray direction are indicated. The two main peaks in the $P(H)$ curve are taken to indicate two regions of different magnetic order in the alloy and the type of order in each is deduced from the way in which the $P(H)$ peaks depend on the applied field ; *b*) $^{121}Sb$ measurements on the alloy $Pd_2MnIn_{0.7}Sb_{0.3}$ at 4.2 K. The magnitudes of the magnetic fields $H_a$ applied perpendicular to the $\gamma$-ray direction are indicated. As for the $^{119}Sn$ results in (a) the two peaks in $P(H)$ are associated with regions of different magnetic order in the sample. The relatively poor statistics of the spectrum run in a magnetic field are due to the large source-detector distance in this configuration and to the relatively low $^{121}Sb$ content of this sample. While care must be taken in the interpretation of $P(H)$ curves derived from spectra of this quality we believe that the two $P(H)$ peaks shown are clearly recognizable in the Mössbauer spectrum : this is our criterion in discussing features of $P(H)$ curves.

perpendicular to the $\gamma$-ray direction. The source was Ca $^{119m}SnO_3$ at room temperature. The $^{121}Sb$ spectra (Fig. 6*b*) are from the isoelectronic alloy $Pd_2MnIn_{0.7}Sb_{0.3}$ also at 4.2 K and with the same experimental geometry. The source was Ca $^{121m}SnO_3$ at $\sim$ 80 K. This source had a satellite line of approximately 9 % of the intensity of the main line and

shifted by $\sim$ 18.7 mm/s with respect to it. This satellite line was included in the fitting of the spectra.

The solid lines drawn through the experimental spectra in figure 6 are those calculated from the corresponding $P(H)$ distributions.

4.2 MAGNETIC HYPERFINE INTERACTION IN $^{121}$Sb MÖSSBAUER SPECTRA. — While the magnetic moment of the ground state of the $^{121}$Sb nucleus is known ($\mu_g = 3.359\,0 \pm 0.000\,2\ \mu_N$ [38]), that of the 37.15 keV excited state is a little uncertain. Ruby [39] showed that the ratio $R$ of the nuclear $g$ factors of the excited ($I = 7/2$) and ground ($I = 5/2$) states is approximately 0.5. Subsequent determinations of $R$ have produced values of 0.533 [40], 0.520 [41] and recently 0.535 [42]. Because of this apparent uncertainty in the exact value of $R$ (we are not entirely convinced of the accuracy of the previous determinations), and because our interest here will be restricted to composition-dependent changes in the gross features of the spectra, we will be satisfied to fit our spectra using the value $R = 0.50$, bearing in mind that the correct value is almost certainly higher than this. The dominant effect of a small change in $R$, to $0.50 + \Delta R$, is to increase the value of the magnetic hyperfine field by a factor of approximately $(1 - 3\,\Delta R)^{-1}$. This must be taken into account in comparing hyperfine field values reported in this paper with those already existing in the literature.

5. **Mössbauer and neutron scattering experiments on $Pd_2MnIn_{1-x}Sn_x$ and $Pd_2MnIn_{1-y}Sb_y$.** — The experiments described in this section provide an example of the complementarity of Mössbauer and neutron elastic scattering measurements in the determination of the magnetic structures of a series of Heusler alloys. The alloys studied were the two isoelectronic series $Pd_2MnIn_{1-y}Sb_y$ ($0 \leqslant y \leqslant 0.5$) and $Pd_2MnIn_{1-x}Sn_x$ ($0 \leqslant x \leqslant 1$) whose end members are antiferromagnetic $Pd_2MnIn$ and the ferromagnet $Pd_2MnSn$ (see [23]). Particularly at the $Pd_2MnIn$ end of the series the structures are known to depend on heat treatment [2] : we will restrict our attention to alloys that have been slow-cooled from high temperatures as these show the largest degree of order in the $L2_1$ structure.

The object of this study was to determine the nature of the magnetic phase change and its dependence on local stoichiometry in the alloy. The neutron results, of course, provide the primary magnetic structure determination. They have been reported [43] and will also be the subject of a forthcoming publication [36]. We summarize the major conclusions below.

5.1 NEUTRON DIFFRACTION RESULTS. — The neutron measurements indicate that two different magnetic phase changes occur in each of the two alloy systems studied. The structures of the phases were identified as being, in the notation of ter Haar and Lines [44], antiferromagnetic type 2 (which will be referred to as A 2) at the $Pd_2MnIn$ end of both series [2], and, as either $Pd_2MnSn$ or $Pd_2MnSb$ were added, the structure changed to antiferromagnetic type 3 A (A 3 A) and finally to ferromagnetic (F). As mentioned in section 2, the magnetic moments were localized at the Mn sites (see also [45]). The spin directions of the Mn ions for the A 2 and A 3 A structures are shown in figure 7*a* and *b*. The magnetic phase, or the proportions of two

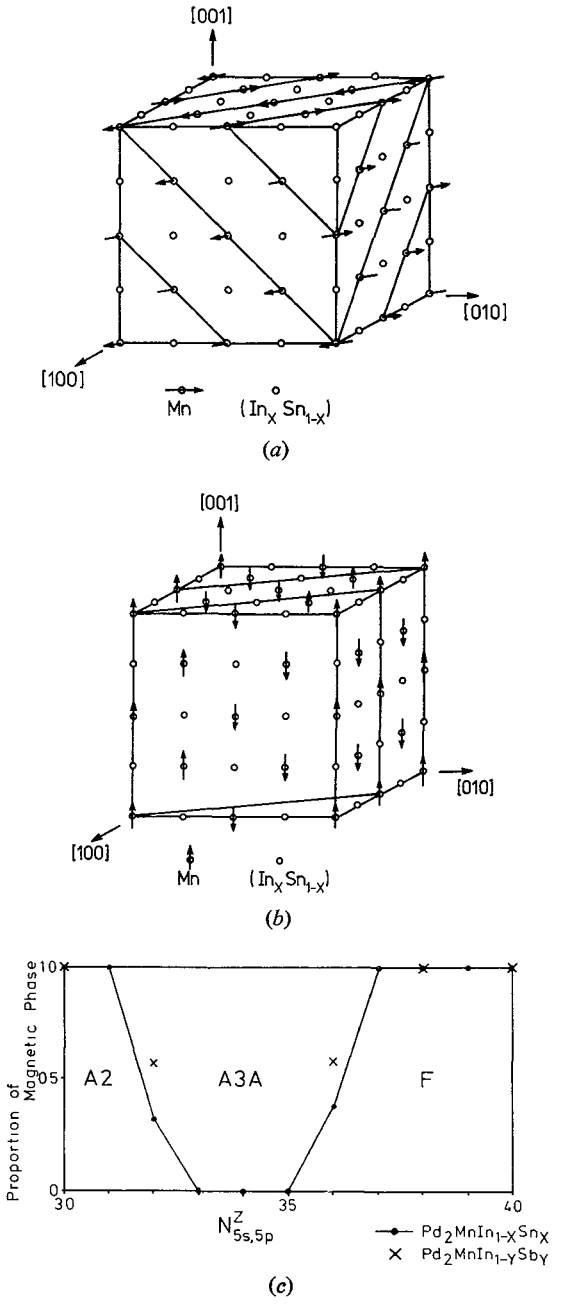


FIG. 7. — Schematic illustration of the antiferromagnetic structures derived from neutron diffraction measurements on $L2_1$ structure alloys in the series $Pd_2MnIn_{1-x}Sn_x$ and $Pd_2MnIn_{1-y}Sb_y$. Only the Mn ions are shown for clarity : *a*) The f. c. c. antiferromagnetic type 2 structure (A 2) [44] ; *b*) The f. c. c. antiferromagnetic type 3 A structure (A 3 A) [44] ; *c*) The magnetic phase diagram derived for these two alloy series. The proportion of each phase existing in an alloy is plotted as a function of $N^Z_{5s,5p}$, the average number of 5s,5p electrons on a Z site ion.

magnetic phases, existing in an alloy were shown to depend on the electron concentration in the alloy, i. e. isoelectronic alloys from the two series studied had the same magnetic structure. It is therefore possible to draw an approximate magnetic phase diagram showing the structure of an alloy as a function of the average number, $N^Z_{5s,\,5p}$, of 5 s, 5 p electrons on a Z site ion, and this is done in figure 7*c*.

5.2 MÖSSBAUER RESULTS. — The $^{119}$Sn Mössbauer results for the series $Pd_2MnIn_{1-x}Sn_x$ and the $^{121}$Sb results for $Pd_2MnIn_{1-y}Sb_y$ are represented by the $P(H)$ curves shown in figures 6, 8 and 9. Those in figure 8 are for the antiferromagnetic alloys, figure 9 contains the

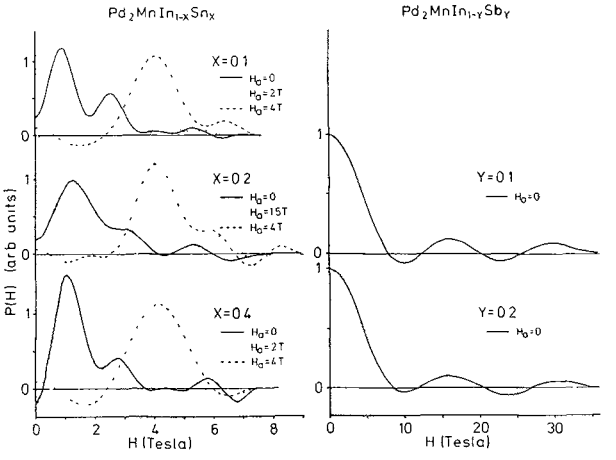


FIG. 8. — $P(H)$ distributions derived from the $^{119}$Sn and $^{121}$Sb Mössbauer spectra of $Pd_2MnIn_{1-x}Sn_x$ and $Pd_2MnIn_{1-y}Sb_y$ alloy at 4.2 K. Results for isoelectronic alloys are on the same horizontal level. Curves for various values of magnetic field $H_a$ applied perpendicular to the $\gamma$-ray direction are shown : all solid curves are from spectra measured in the absence of an applied field. The changes in the peak positions of the $^{119}$Sn $P(H)$ distributions with applied field indicate that these alloys are antiferromagnetic, as deduced from neutron diffraction measurements.

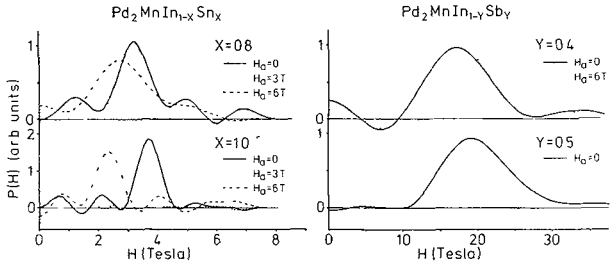


FIG. 9. — $P(H)$ distributions derived from the $^{119}$Sn and $^{121}$Sb Mössbauer spectra of $Pd_2MnIn_{1-x}Sn_x$ and $Pd_2MnIn_{1-y}Sb_y$ alloys at 4.2 K. Results for isoelectronic alloys are on the same horizontal level. Curves for various values of magnetic field $H_a$ applied perpendicular to the $\gamma$-ray direction are shown : all solid curves are from spectra measured in zero applied field. The changes in the peak positions of the $P(H)$ distributions with applied field indicate that these alloys are ferromagnetic as deduced from neutron diffraction measurements.

results for the ferromagnetic alloys whilst figure 6 shows the spectra of alloys of mixed F and A 3 A phases. The $P(H)$ curves in figures 8 and 9 are arranged so that results for isoelectronic alloys are on the same horizontal level.

The main features of the results for the antiferromagnetic alloys in zero applied field (Fig. 8) are a broad peak near $H = 1$ T and a smaller peak near 3 T in the $^{119}$Sn spectra, and a broad peak near $H = 0$ in the $^{121}$Sb spectra. One observation that can be made is that there appears to be no significant difference in the results for alloys of A 2 and A 3 A structure, and this is consistent with the structures. In both structures (see Fig. 7*a* and *b*) every co-ordination shell of Mn ions around a Z site contains equal numbers of moments in each direction. However, this would lead us to expect zero hyperfine field at the Z site nuclei in both structures. We are not certain why the main peak of the $^{119}$Sn spectra occurs at $\sim$ 1 T rather than at $H = 0$ but a similar result was obtained for $FeSn_2$ [46]. The results of figure 8 clearly do not preclude the possibility of a similar field being present at the $^{121}$Sb nuclei in the antiferromagnetic $Pd_2MnIn_{1-y}Sb_y$ alloys because the peaks in the $P(H)$ curves are much broader than 1 T. This peak width may be ascribed to a number of causes including the use of a relatively small number of harmonics to describe the $P(H)$ function, the presence of small unresolved quadrupole interactions, and metallurgical disorder in the alloys. In particular, Mn-In disorder is known to exist, even in slow-cooled alloys, at the $Pd_2MnIn$ end of both alloy series [2], [36], [43]. We attribute the smaller peaks near 3 T in the $P(H)$ at $^{119}$Sn nuclei in $Pd_2MnIn_{1-x}Sn_x$ to the presence of the disordered B 2 phase.

When an external magnetic field $H_a$ is applied, the peak at $H_0 \sim 1$ T in the $^{119}$Sn $P(H)$ curves moves roughly as $\sqrt{H_0^2 + H_a^2}$ (Fig. 8) as would be expected for a cubic antiferromagnet with the internal field $H_0$ parallel to the direction of the Mn magnetic moments.

The results for the isoelectronic alloys $Pd_2MnIn_{0.4}Sn_{0.6}$ and $Pd_2MnIn_{0.7}Sb_{0.3}$ given in figure 6 are of particular interest. The two large peaks in both the $^{119}$Sn and $^{121}$Sb $P(H)$ curves indicate the presence of two separate well-defined environments for the Z site ions. The magnetic phase diagram for the systems (Fig. 7*c*) shows that the F and A 3 A phases are present in both of these alloys, and we assign the two $P(H)$ peaks in each case to Z site ions in F and A 3 A magnetic regions of the crystals. Comparison with the results of figures 8 and 9 leads us to associate the higher field $P(H)$ peak in each case to nuclei in ferromagnetic regions. The applied field dependences are consistent with this assignment. The area ratios of the two $P(H)$ peaks in each case appear to be qualitatively similar to the proportions of the two phases present in the respective alloys (Fig. 7*c*). Therefore, when considered together in this way, the Mössbauer and neutron results appear to indicate that

the A 3 A-F magnetic phase boundary in these alloys depends very sensitively on the average density of s, p electrons in a region of crystal, and that two phases can occur in a single sample because of rather small (probably statistical) fluctuations in this electronic density within the crystal. The coexistence of two magnetic phases cannot be associated with any metallurgical segregation in the alloy.

The results for the ferromagnetic alloys in the range under consideration (i. e. $x \leqslant 1, y \leqslant 0.5$) are illustrated by the $P(H)$ curves in figure 9. The curves for both $^{119}$Sn and $^{121}$Sb nuclei show one main peak, broadened perhaps by quadrupole interactions and disorder effects. The linear dependence of the peak positions on applied field indicates that the alloys are fairly isotropic ferromagnets, and shows that the $^{119}$Sn hyperfine field in the (In, Sn) alloy series is negative (antiparallel to the magnetization direction) while that at $^{121}$Sb nuclei in the (In, Sb) series is positive. The former result agrees with previously reported results for $Pd_2MnSn$ [47] and both agree qualitatively with the hyperfine field systematics discussed above (Section 3).

5.3 Discussion. — The Mössbauer results for both alloy systems discussed above are qualitatively consistent with the magnetic structures deduced from neutron diffraction measurements and summarized in figure 7, although we could not distinguish between the two antiferromagnetic phases.

The fact that the magnetic structures of the two alloy systems can be represented on a phase diagram such as figure 7*c* as a unique function of the average s, p electron density shows that this density plays a crucial role in determining the nature of the magnetic order in these systems. The Mössbauer results presented here indicate further a rather strong sensitivity of the magnetic phase to the local conduction electron density : two well-defined and quite distinct magnetic structures were observed in a single sample with no evidence for anything but small statistical fluctuations in the electron density throughout the crystal.

It is tempting to interpret this as evidence that the dominant exchange mechanism is the long-range double resonance process discussed in section 2. Magnetic phase changes would then occur as a result of expansion or contraction of the $J(r)$ curve (Fig. 2) due to changes in the value of $k_F$. Darby and Webster [48] have calculated the most stable magnetic phase for various values of $k_F$ and of the Mn moment using the asymptotic Caroli-Blandin [4] expressions for the double resonance interaction. In a similar way we have calculated the magnetic transition temperature for various magnetic phases as a function of $k_F$ using a molecular field approximation and taking the exchange integral to be as calculated in section 2 and shown as the solid line in figure 2, since this particular curve represents the experimental data for $Pd_2MnSn$ quite well. In terms of this effective exchange integral $J(r)$, the magnetic transition temperature is given in the molecular field approximation as :

$$k_B T_c = \frac{2}{3} S(S+1) \sum_{i=1}^{N} \gamma_i J(r_i) \qquad (5)$$

where $k_B$ is the Boltzmann constant, $\gamma_i$ is the net number of Mn moments in the $i^{th}$ co-ordination shell at a radial distance $r_i$ from the Mn moment at the origin. The summation in (5) was extended over $N = 12$ shells, to include a total of 248 Mn neighbours. The results of this calculation for four different magnetic structures (F, A 2, A 3 A, A 3 B — see [44]) are shown in figure 10. They indicate that a small decrease in $k_F$ from its value in $Pd_2MnSn$ can explain quite complex changes in the magnetic structure. Using these results we would predict a change from A 2 → A 3 B → F order as $k_F$ is increased towards its value in $Pd_2MnSn$, whereas the observed sequence is A 2 → A 3 A → F. In view of the approximations involved in the molecular field model, the calculated radial dependence of the effective exchange integral (see Section 2) and truncation of the summation in eq. (5) at $N = 12$ (see [5]) we do not regard the difference between the experimental results and those shown in figure 10 as necessarily indicating the existence of other large exchange processes. Neither of the other mechanisms proposed ([10], [12]) could correct the predicted sequence of structures.

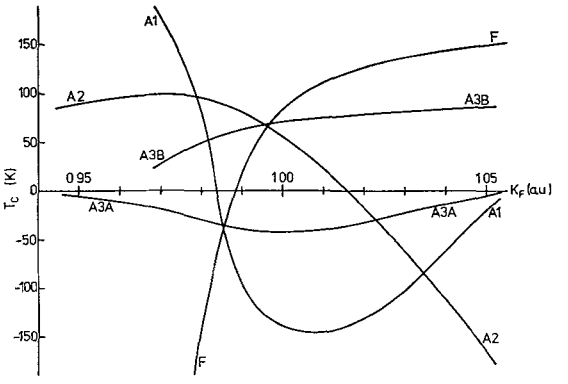


Fig. 10. — The magnetic transition temperature $T_c$ as a function of the effective value of $k_F$ calculated for the various magnetic structures indicated (see [44]) using the molecular field model described in the text and the exchange interaction shown by the solid line in figure 2. From this it would be predicted that, with increasing $k_F$, the magnetic structure would change from A2 → A3B → F.

**6. Mössbauer measurements on alloys near the $Pd_2MnSb$ composition.** — Recent measurements of the hyperfine fields at the nuclei of 5s, p elements substituted into the Z site in $Pd_2MnSb$ give results that are, in most cases, significantly more positive than expected on the basis of the models described in section 3 ([49], [42], [50] [51], [52], [53]). In order to examine the applicability of these models in this case we

have made both $^{119}$Sn and $^{121}$Sb Mössbauer measurements on alloys in the series $Pd_2MnSb_{1-x}Sn_x$ ($0 \leqslant x \leqslant 1$), $Pd_2MnSb_{1-y}In_y$ ($0 \leqslant y \leqslant 0.5$) and $Pd_{1+z}MnSb$ ($0 \leqslant z \leqslant 1$). These measurements indicate that the application to $Pd_2MnSb$ of the hyperfine field models discussed in section 3 is not straight forward, possibly because of strong deviations from free electron-like behaviour of the conduction electrons.

6.1 $^{121}$Sb MÖSSBAUER RESULTS FOR $Pd_2MnSb_{1-x}Sn_x$ AND $Pd_2MnSb_{1-y}In_y$. — $P(H)$ distributions derived from $^{121}$Sb Mössbauer spectra of the $L2_1$ structure alloys $Pd_2MnSb_{1-x}Sn_x$ and $Pd_2MnSb_{1-y}In_y$ are shown in figure 11. Results for isoelectronic alloys from each

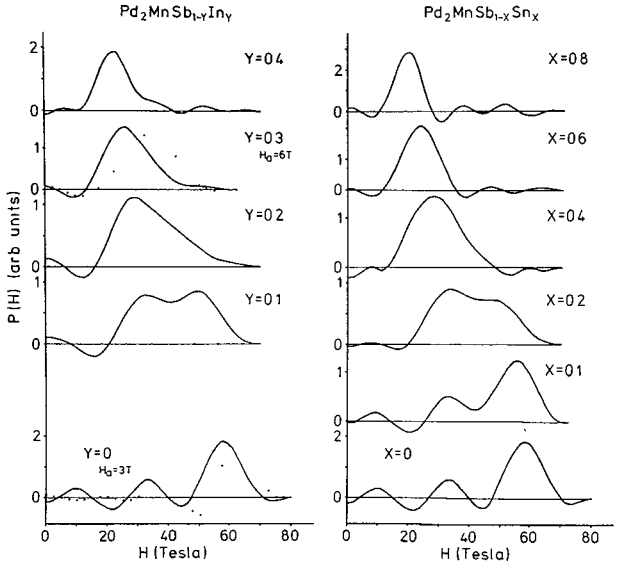


FIG. 11. — $P(H)$ distributions derived from the $^{121}$Sb Mössbauer spectra of $Pd_2MnSb_{1-y}In_y$ and $Pd_2MnSb_{1-x}Sn_x$ alloys at 4.2 K. Results for isoelectronic alloys are on the same horizontal level. Curves for various values of magnetic field $H_a$ applied perpendicular to the $\gamma$-ray direction are shown : all solid curves are from spectra measured in zero applied field. The changes in the peak positions of the $P(H)$ distributions with applied field confirm that these alloys are ferromagnetic and that the $^{121}$Sb hyperfine fields are in the same direction as the alloy magnetization (i. e. are positive).

series are on the same horizontal level. Firstly, it can be seen that the distributions in isoelectronic alloys are very similar, which indicates that electronic density is an important parameter in determining the hyperfine field, as is expected from the discussion of section 3. The second feature of significance is the way in which the probability distribution changes from a single peak near $H = 20$ T for low electron densities ($x \to 1$, $y \to 0.5$) to a single peak near 60 T for pure $Pd_2MnSb$. It is an important point that this change is not achieved by a simple shift of the single peak but mainly by the probability being redistributed through a series of broad, but apparently well-defined, peaks. We interpret this as indicating a strong sensitivity of the electronic spin polarization at a Z site to local fluctuations in the conduction electron density. In terms of the hyperfine field models discussed in section 3 this would imply a strong dependence either of the effective value of $k_F$ or of the conduction band polarization (or both) on the local environment of a Z site ion. Such an interpretation is not consistent with simple free electron-like behaviour of the conduction electrons.

6.2 $^{119}$Sn MÖSSBAUER RESULTS FOR $Pd_2MnSb_{1-x}Sn_x$. — Figure 12 shows the $^{119}$Sn Mössbauer results for the alloys in this series whose $^{121}$Sb spectra were represent-

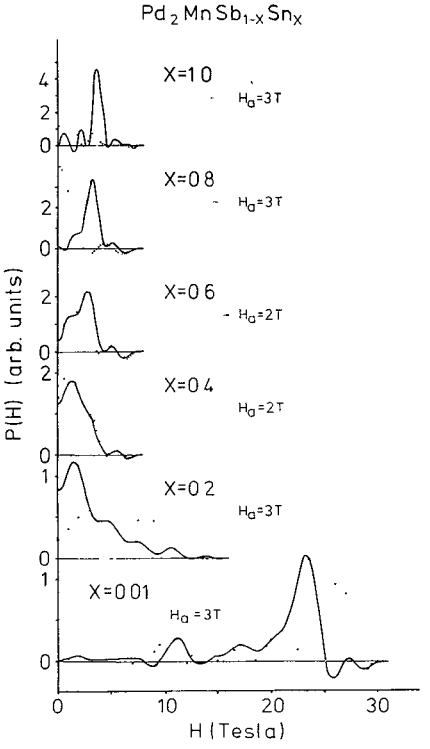


FIG. 12. — $P(H)$ distributions derived from the $^{119}$Sn Mössbauer spectra of $Pd_2MnSb_{1-x}Sn_x$ alloys at 4.2 K. Curves for various values of magnetic field $H_a$ applied perpendicular to the $\gamma$-ray direction are shown : all solid curves are from spectra measured in zero applied field. The changes in the peak positions of the $P(H)$ distributions with applied field confirm that these alloys are ferromagnetic and that the $^{119}$Sn hyperfine fields are negative for large values of $x$ and become positive as $x$ is decreased.

ed in figure 11, and qualitatively similar behaviour is observed. The $^{119}$Sn $P(H)$ distribution changes from a single peak at $H \sim -3.7$ T in $Pd_2MnSn$ through a series of strongly broadened peaks to a single peak at $H \sim +23$ T for $Pd_2MnSb_{0.99}Sn_{0.01}$. The alloys whose spectra are shown here (and in Fig. 13) were quenched rapidly from $\sim 800$ °C, but slow-cooling gave qualitatively similar results. It may be noted that the $P(H)$ curves derived from $^{119}$Sn Mössbauer spectra appear to be better resolved in some cases than those from $^{121}$Sb spectra. This is partly because of a difference in nuclear properties (excited state lifetime, ground and excited state magnetic moments) and

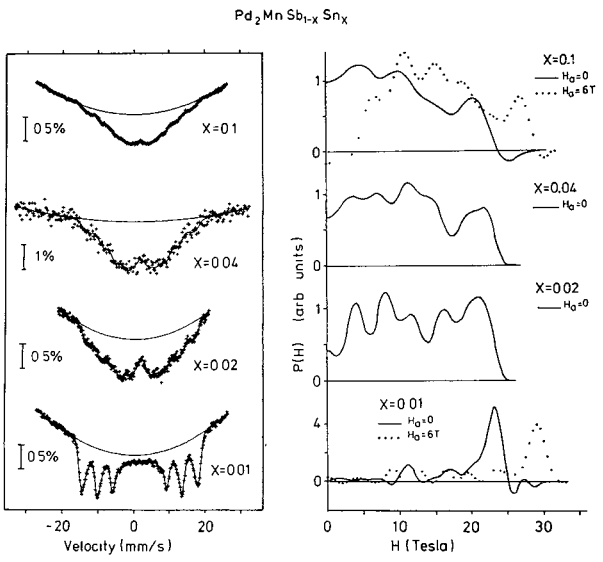


FIG. 13. — $^{119}$Sn Mössbauer spectra and $P(H)$ distributions derived from them for $Pd_2MnSb_{1-x}Sn_x$ alloys in the range $0.01 \leqslant x \leqslant 0.10$ at 4.2 K. The spectra shown were measured in zero applied field and the $P(H)$ distributions derived from them are the solid curves. The $P(H)$ curves derived from spectra (not shown) that were measured with fields of 6 T applied perpendicular to the $\gamma$-ray direction indicate that the $^{119}$Sn hyperfine fields are mostly positive.

partly because the hyperfine fields at $^{119}$Sn nuclei are normally smaller in magnitude than those observed at $^{121}$Sb nuclei.

The composition region near $Pd_2MnSb$ is examined in more detail in figure 13. On the basis of the composition dependence observed we would associate the peak in the $P(H)$ distribution at $\sim +23$ T with $^{119}$Sn nuclei that are isolated from the effects of other Sn ions in the $Pd_2MnSb$ host. This is in general agreement with the results of Boolchand *et al.* [52], but is in marked disagreement with a previously reported measurement of Campbell and Leiper [21].

If the interpretation given above for the $^{121}$Sb results is applied to the results of figure 13 it would seem necessary to further conclude that, for concentrations of the order of 2 % or less, tin ions do not substitute for Sb ions in a random manner, although it is not clear whether this is due to an effective attraction or repulsion between Sn ions. If the interaction was attractive it would need to be of sufficiently short range to be virtually ineffective in $Pd_2MnSb_{0.99}Sn_{0.01}$, whereas if it was repulsive then the broad multi-peaked nature of the $P(H)$ distribution for $^{119}$Sn in $Pd_2MnSb_{0.98}Sn_{0.02}$ would imply that the hyperfine field at a $^{119}$Sn nucleus can be quite strongly affected by a fairly distant Sn neighbour. However, these results could also be interpreted as implying a concentration-dependent non-randomness in the distribution of tin atoms in the Z sites that may originate in band-structure effects which we believe may also be responsible for the large hyperfine field variations observed. There does not appear to be any evidence for non-random substitution in more concentrated alloys. A previous example of the detection of non-random substitution in solid solutions by hyperfine interaction measurements has been reported [54].

Figure 14 shows $^{119}$Sn spectra for the $Pd_2MnSb_{0.98}Sn_{0.02}$ alloy at temperatures of 226 K, 235 K and 240 K. It is apparent from them that the $^{119}$Sn ions are in an environment of reasonable magnetic homogeneity with a mean Curie temperature somewhere between 235 and 240 K. We will see below (Section 6.4) that this is consistent with the Heusler phase $Pd_2MnSb_{1-x}Sn_x$ and appears to preclude the possibility that a significant fraction of the Sn atoms are in an impurity phase.

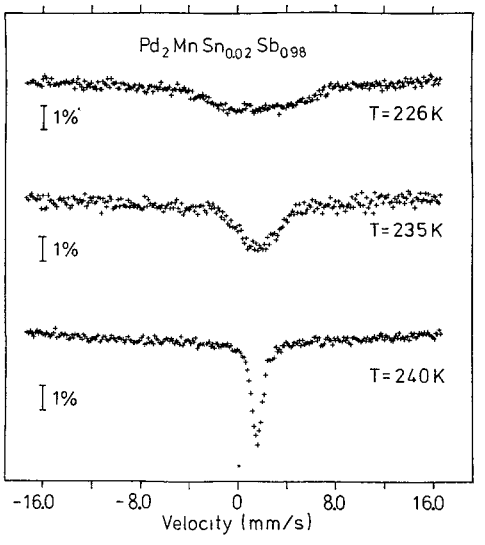


FIG. 14. — $^{119}$Sn Mössbauer spectra for the $Pd_2MnSb_{0.98}Sn_{0.02}$ alloy at 226 K, 235 K and 240 K showing the collapse of the spectra from well split, although poorly resolved, magnetic hyperfine structure to a narrow single line within a small temperature range.

6.3 $^{121}$Sb MÖSSBAUER MEASUREMENTS ON $Pd_{1+z}MnSb$. — Hyperfine field probability distributions derived from the $^{121}$Sb Mössbauer spectra of $Pd_{1+z}MnSb$ alloys (for $0 \leqslant z \leqslant 1$) are shown in figure 15 along with those for the isoelectronic series $Ni_{1+z}MnSb$. Similar results have been reported earlier by Swartzendruber and Evans [22], [33]. Our intention is to point out the differences in the results for the two systems and the qualitative similarity of the $Pd_{1+z}MnSb$ results with those from the $Pd_2Mn(Sb, Sn)$ and $Pd_2Mn(Sb, In)$ series shown in figure 11. In making this latter comparison we do not wish to make a detailed examination of the apparently equivalent effects of removing Pd atoms from $Pd_2MnSb$ and substituting Sn or In atoms for Sb, but simply to draw attention to the qualitatively similar way in which the $^{121}$Sb hyperfine field appears to depend quite strongly on local atomic environment. This can again be inter-

preted to indicate that the spin polarization at a $^{121}$Sb site in alloys near to the composition $Pd_2MnSb$ is very sensitive to local electron density fluctuations. It is not clear how such a sensitivity could be explained in terms of the usual assumption (e. g. [17], [10]) that Pd (and Ni) atoms contribute only about 0.1 electrons to a free electron-like conduction band in the alloy. The results for $^{121}$Sb in $Ni_{1+z}MnSb$ (Fig. 15) show that

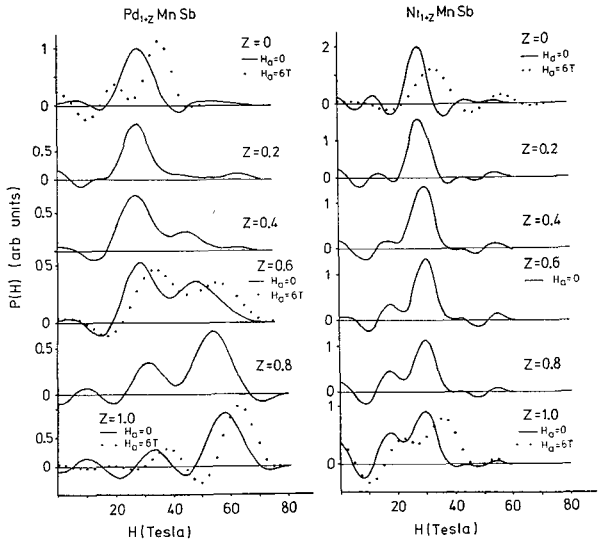


FIG. 15. — $P(H)$ distributions derived from the $^{121}$Sb Mössbauer spectra of $Pd_{1+z}MnSb$ and $Ni_{1+z}MnSb$ alloys at 4.2 K. The solid curves are from spectra measured in zero applied field while the dotted curves are from spectra measured when a field of 6 T was applied perpendicular to the $\gamma$-ray direction. These confirm that the alloys are ferromagnetic and indicate that the $^{121}$Sb hyperfine fields are positive.

most $^{121}$Sb nuclei experience a hyperfine field that is essentially independent of Ni concentration, which is in better agreement with this assumption. The appearance of a subsidiary peak in the $^{121}$Sb $P(H)$ curve for $z \gtrsim 0.5$ has been attributed to Mn-Ni disorder [49].

6.4 CURIE TEMPERATURES. — Figure 16 shows the Curie temperatures [36], [43] for the ferromagnetic alloys in the series $Pd_2MnIn_{1-x}Sn_x$ and $Pd_2MnSb_{1-x}Sn_x$ plotted as a function of $N^z_{5s,5p}$, the average number of 5s, 5p electrons on a Z site ion. For smaller values of $N^z_{5s,5p}$ the Curie temperature increases gradually and then flattens out with increasing number of electrons in a way that is qualitatively similar to that predicted by the molecular field model (Fig. 10). However, as $Pd_2MnSb$ is approached the Curie temperature starts to increase quite rapidly. This behaviour cannot be explained in terms of the simple molecular field model unless the occupied part of the conduction band is changing significantly near $Pd_2MnSb$, as has been suggested above.

Another point of interest concerns the pressure dependence of $T_c$. Austin and Mishra [55] measured

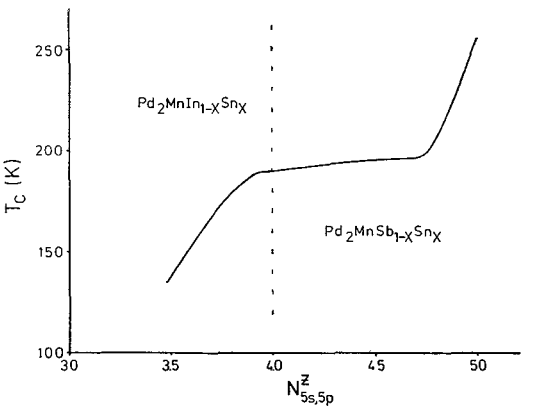


FIG. 16. — The Curie temperatures of ferromagnetic alloys in the two series $Pd_2MnIn_{1-x}Sn_x$ and $Pd_2MnSb_{1-x}Sn_x$ plotted as a function of $N^z_{5s,5p}$, the average number of 5s, 5p electrons on a Z site ion.

this quantity for $Pd_2MnSn$ and $Pd_2MnSb$ and attributed the « striking variation » between the two to conduction band differences.

6.5 DISCUSSION. — It is clear from the broad, multiple-peaked nature of the $P(H)$ curves in figures 11, 12, 13 and 15 that in alloys near the $Pd_2MnSb$ composition the hyperfine field at a Z site nucleus depends strongly on its local environment. We have interpreted this to indicate a strong dependence of the local electronic structure on environment. This is in marked contrast to the results presented in section 5 which could be described in terms of the average electronic density. We suggest that the difference here is either that there are important structural features in the conduction band near to the Fermi surface, or that the nature of the electronic screening of the Pd ion is strongly dependent on local environment. In this context it may be noted that the NMR results of Endo *et al.* [56] for the system $Ni_{1-x}Cu_xMnSb$ indicate $^{121}$Sb $P(H)$ distributions that are remarkably similar to those reported here for $x \lesssim 0.5$ (see also [57]).

Finally, it may be noted that the results presented in this section cannot be reconciled in any reasonable way with a model for the origin of the hyperfine field that depends largely on atomic volume effects, such as that proposed by Stearns [24]. Consequently we assume that electronic effects are important in determining the hyperfine fields at non-magnetic ions in Heusler alloys.

7. **Conclusions.** — We have tried to summarize the present level of understanding of the magnetic properties of the $X_2MnZ$ Heusler alloys and of the origins of the hyperfine interactions at Z site nuclei. It is mainly based on experimental measurements and on phenomenological models derived from them. It is our feeling that there is now sufficient information available to justify more detailed theoretical work being undertaken

and we believe that further significant advances in understanding will require a more rigorous theoretical basis with which to compare experimental results. For reasons given in sections 2 and 3, we believe that the continuation of carefully planned experimental work designed to test the fundamental principles of phenomenological models is likely to be more worth while than further testing of the fine numerical details of these models.

**Acknowledgments.** — We wish to thank P. Jena for interesting discussions.

JDR wishes to acknowledge the receipt of a Research Studentship from the Science Research Council.

## References

[1] WEBSTER, P. J., *Contemp. Phys.* **10** (1969) 559.
[2] WEBSTER, P. J. and TEBBLE, R. S., *Phil. Mag.* **16** (1967) 347.
[3] CAMPBELL, C. C. M., *J. Phys. F.* **5** (1975) 1931.
[4] CAROLI, B. and BLANDIN, A., *J. Phys. & Chem. Solids* **27** (1966) 503.
[5] GELDART, D. J. W. and GANGULY, P., *Phys. Rev.* **B 1** (1970) 3101.
[6] BROOKS, J. S. and WILLIAMS, J. M., *J. Phys. F.* **4** (1974) 2033.
[7] CAROLI, B., *J. Phys. & Chem. Solids* **28** (1967) 1427.
[8] ANDERSON, P. W., *Phys. Rev.* **124** (1961) 41.
[9] ISHIKAWA, Y. and NODA, Y., *Solid State Commun.* **15** (1974) 833.
ISHIKAWA, Y. and NODA, Y., *A. I. P. Conf. Proc.* n° 24 (1975) 145.
NODA, Y. and ISHIKAWA, Y., *J. Phys. Soc. Japan* **40** (1976) 690.
[10] KASUYA, T., *Solid State Commun.* **15** (1974) 1119.
[11] CAMPBELL, C. C. M. and STAGER, C. V., *Can. J. Phys.* (to be published).
STAGER, C. V. and CAMPBELL, C. C. M., *Can. J. Phys.* (to be published).
[12] CAMPBELL, C. C. M., private communication, to be published.
[13] GOODENOUGH, J. B., *Magnetism and the Chemical Bond* (Wiley, New York) 1963.
[14] MORIYA, T., in *Theory of Magnetism in Transition Metals*, ed. W. Marshall (Academic, New York) 1967.
[15] KIM, D. J. and NAGAOKA, Y., *Prog. Theor. Phys.* **30** (1963) 743.
[16] ALLOUL, H., *J. Phys. F.* **4** (1974) 1501.
[17] JENA, P. and GELDART, D. J. W., *Solid State Commun.* **15** (1974) 139.
[18] HEEGER, A. J., in *Solid State Physics* eds. H. Ehrenreich, F. Seitz and D. Turnbull (Academic, New York) 1969, Vol. 23.
[19] GRÜNER, G., *Adv. Phys.* **23** (1974) 941.
[20] LEIPER, W. and CAMPBELL, C. C. M., reported in *Perspectives in Mössbauer Spectroscopy*, eds. S. G. Cohen and M. Pasternak (Plenum, New York) 1973.
[21] CAMPBELL, C. C. M. and LEIPER, W., *A. I. P. Conf. Proc.* n° 18 (1973) 319.
[22] SWARTZENDRUBER, L. J. and EVANS, B. J., *A. I. P. Conf. Proc.* n° 10 (1972) 1369.
[23] DANIEL, E. and FRIEDEL, J., *J. Phys. & Chem. Solids* **24** (1963) 1601.
[24] STEARNS, M. B., *Phys. Lett.* **34A** (1971) 146.
STEARNS, M. B., *Phys. Rev.* **B 4** (1971) 4081.
STEARNS, M. B., *Phys. Rev.* **B 8** (1973) 4383.
[25] BLANDIN, A. and CAMPBELL, I. A., *Phys. Rev. Lett.* **31** (1973) 51.
CAMPBELL, I. A. and BLANDIN, A., *J. Mag. Mag. Mat.* **1** (1975) 1.
[26] STEARNS, M. B., private communication to W. Leiper.
[27] CAMPBELL, I. A. and VINCZE, I., *Phys. Rev.* **B 13** (1976) 4178.
[28] STEARNS, M. B., *Phys. Rev.* **B 13** (1976) 4180.
[29] MÖLLER, H. S., *Solid State Commun.* **8** (1970) 527.
[30] LE DANG KHOI, VEILLET, P. and CAMPBELL, I. A., *J. Phys. F.* **5** (1975) 2184.
[31] SONDHI, I., *J. Chem. Phys.* **62** (1975) 1385.
[32] JENA, P. and GELDART, D. J. W., private communication, to be published.
[33] SWARTZENDRUBER, L. J. and EVANS, B. J., *A. I. P. Conf. Proc.* n° 5 (1971) 539.
[34] WATSON, R. E. and BENNETT, L. H., preprint, Brookhaven National Laboratory n° BNL-21690 (1976).
[35] KOENIG, C., *J. Phys. F.* **3** (1973) 1497.
[36] WEBSTER, P. J. and RAMADAN, M. R. I., to be published.
[37] WINDOW, B., *J. Phys. E.* **4** (1971) 401.
[38] See *Mössbauer Effect Data Index*, eds. J. G. Stevens and V. E. Stevens (Plenum, New York) 1973.
[39] RUBY, S. L., *Mössbauer Effect Methodology* **3** (1967) 203.
[40] RUBY, S. L. and KALVIUS, G. M., *Phys. Rev.* **155** (1967) 353.
RUBY, S. L. and JOHNSON, C. E., *Phys. Lett.* **26A** (1967) 60.
[41] IKRAEV, S. M., VALIEV, K. K., GOLOVNIN, V. A. and KUZ'MIN, R. N., *Zh. Eksp. Teor. Fiz.* **59** (1970) 419 (*Sov. Phys.-J. E. T. P.* **32** (1971) 229).
[42] LANGOUCHE, G., DIXON, N. S., MAHMUD, Y., TRIPLETT, B. B., HANNA, S. S. and BOOLCHAND, P., *Phys. Rev.* **C 13** (1976) 2589.
[43] RAMADAN, M. R. I., Ph. D. Thesis, University of Salford, U. K. (1975).
[44] TER HAAR, D. and LINES, M. E., *Philos. Trans. R. Soc.* **254A** (1962) 521.
[45] NODA, Y. and ISHIKAWA, Y., *J. Phys. Soc. Japan* **40** (1976) 699.
[46] TRUMPY, G., BOTH, E., DJEGA-MARIADASSOU, C. and LECOCQ, P., *Phys. Rev.* **B 2** (1970) 3477.
[47] GELDART, D. J. W., CAMPBELL, C. C. M., POTHIER, P. J. and LEIPER, W., *Can. J. Phys.* **50** (1972) 206.
[48] DARBY, M. I. and WEBSTER, P. J., in 21st Annual Conference on Magnetism and Magnetic Materials, Philadelphia, Dec. 1975 (to be published in *A. I. P. Conf. Proc.*).
[49] SWARTZENDRUBER, L. J. and EVANS, B. J., *Phys. Lett.* **38A** (1972) 511.
[50] BOOLCHAND, P., TENHOVER, M., JHA, S., LANGOUCHE, G., TRIPLETT, B. B., HANNA, S. S. and JENA, P., *Phys. Lett.* **54A** (1975) 293.
[51] MACKAY, G. R., BLAAUW, C. and LEIPER, W., *J. Phys. F.* **5** (1975) L 166.
[52] BOOLCHAND, P., TENHOVER, M., JHA, S., LANGOUCHE, G., TRIPLETT, B. B. and HANNA, S. S., *Solid State Commun.* (to be published).
[53] CAMPBELL, C. C. M. and CAMERON, J. A., *J. Phys. F.* **6** (1976) L 221.
[54] LE DANG KHOI, VEILLET, P. and CAMPBELL, I. A., *J. Phys. F.* **4** (1974) 2310.
[55] AUSTIN, I. G. and MISHRA, P. K., *Phil. Mag.* **15** (1967) 529.
[56] ENDO, K., SHINOGI, A. and KIMURA, R., *J. Phys. Soc. Japan* **34** (1973) 268.
[57] SWARTZENDRUBER, L. J. and EVANS, B. J., *J. Phys. Colloq.* **35** (1974) C 6-265.